Delamination growth analysis of composite panels

Werner Wagner* — **Friedrich Gruttmann****

* *Institut für Baustatik, Universität Karlsruhe (TH)*
Kaiserstraße 12
D-76131 Karlsruhe
ww@bs.uka.de

** *Institut für Werkstoffe und Mechanik im Bauwesen, TU Darmstadt*
Petersenstraße 12
D-64287 Darmstadt
gruttmann@iwmb.tu-darmstadt.de

ABSTRACT. *The present paper deals with the numerical simulation of delamination in composite panels. Within our model interface layers are positioned at layer boundaries where damage is expected. The material model considering inelastic strains is written in terms of the Green–Lagrangian strains and work–conjugated 2^{nd}Piola Kirchhoff stress tensor. The delamination criterion of Hashin is reformulated as a yield criterion with softening. The critical energy release rate controls the delamination process. Refined hexahedral elements are used to discretize laminated structures. To avoid mesh dependent solutions a special regularization technique is applied. Additional viscous strain rates are superposed onto the rate independent model. Parameter studies show the influence of the different constitutive and numerical quantities. Furthermore we investigate the influence of delamination on the stability of composite plates.*

RÉSUMÉ. *Ce papier concerne la simulation numérique du délaminage des panneaux composites. Dans notre modèle les interfaces sont positionnées à priori là ou l'endommagement est attendu. Le modèle est formulé en déformations de Green Lagrange et contraintes de Piola Kirchoff de seconde espèce. Le modèle de délamination d'Hashin est reformulé comme un critère de plasticité avec adoucissement. Le taux de restitution critique d'énergie contrôle le processus de délamination. Des hexahedres sophistiqués sont utilisés pour discrétiser les structures délaminées. Une technique spéciale de régularisatioon est appliquée pour éviter la dépendance au maillage. Pour ce faire on ajoute une contrainte visqueuse. Une analyse paramétrique permet de comprendre l'influence des paramêtres du modèle. Enfin on étudie l'infleunce de la délamination sur le flambage des plaques composites.*

KEYWORDS: *Composite laminates, delamination, viscoplasticity, finite elements*

MOTS-CLÉS : *délamination, viscoplasticité, éléments finis, composites stratifiés*

Revue européenne des éléments finis. Volume 13 - n° 8/2004, pages 915 to 929

1. Introduction

Laminated shells are often used in light weighted structures. High strength and stiffness ratios are the main advantages of these materials. We consider carbon fiber or glass fiber reinforced polymers. A complicated interaction of the different failure modes can be observed in experiments. Especially delamination may lead to a significant reduction of the carrying load and to a reduction of lifetime under dynamic loading. Under compressive loads the process is driven by buckling of the sublaminate. Usually numerical tools like the finite element method are applied to simulate the complicated structural behaviour.

Several authors use stress–based criteria to predict different failure modes. The so–called first–ply failure analysis yields the location where damage starts. Stiffness parameters are reduced or set to zero if the criterion is not fulfilled. Especially within geometrical nonlinear calculations the equilibrium iterations may become unstable. Other authors apply so–called virtual crack–extension or crack–closure methods. When the energy related to the newly opened crack-surface exceeds a critical value, the delamination propagates. The energy release rate can be calculated using the nodal forces and displacements of a finite element solution, see e.g. Wang et.al.[WAN85]. In some papers interface elements with double nodes are used to map the geometric discontinuities arising within the delamination process, see e.g. Schellekens and de Borst [SCH94]. The authors develop plane strain elements and associated interface elements with cubic interpolation functions. The constitutive equations for the interface element are formulated using the crack opening displacements. Crisfield et al. [CRIS97] modified the concept along with eight–node quadrilateral plane strain elements.

In this paper we present a finite element tool for the prediction of damage in layered structures. Especially the influence of delaminations on the stability behaviour of composite panels is investigated. The developed hexahedral shell element is able to predict the three–dimensional stress state, which typically occurs in composite structures. Based on mixed variational principles special interpolation techniques are applied. The transverse shear strains are approximated according to the paper of Dvorkin and Bathe [BAT84]. For the normal strains in thickness direction we consider the shape functions of Betsch and Stein [BET95]ANS-method. Both type of interpolations are performed in the middle plane of the element. The membrane behaviour is essentially improved applying the enhanced strain method (EAS) with five parameters. Due to the different shape functions the element orientation must be considered when generating the mesh. Detailed finite element equations of the ANS–EAS5–element are given in Klinkel, Gruttmann and Wagner[KLI99].

Delamination of layered composites usually occurs together with damage within the plies. However, the complicated interaction between the different failure modes is not investigated in the paper. We introduce interface elements with small but not vanishing thickness. Here, the three–dimensional stress state follows from an inelastic material law. For this purpose the delamination criterion of Hashin is reformulated

as a yield criterion with softening. The slope of the softening curve is determined with the critical energy release rate, the thickness of the interface layer and the tensile strength of the laminate in thickness direction. Complete delamination is given if the newly opened surface is free of stresses. Mesh dependent solutions are avoided using a viscoplastic regularization. The variational formulation is written in a material formulation in terms of the Second Piola–Kirchhoff stress tensor and the work conjugate Green–Lagrangian strain tensor. The tensor components refer to different basis systems, where the transformations are specified in Sprenger, Gruttmann and Wagner[SPR00].

The main aspect of the present paper is the investigation of stability problems with propagating delamination in contrast to results in [SPR00] where stationary delaminations have been considered.

2. Delamination Model

2.1. *Interface layer*

We position interface layers with thickness h_t in those regions where delamination is expected, see Fig. 1. The thickness is chosen as $h_t \approx 10^{-2}\, h$, where h denotes the total thickness of the laminate. With these thickness ratios the global structural behaviour remains practically unaltered.

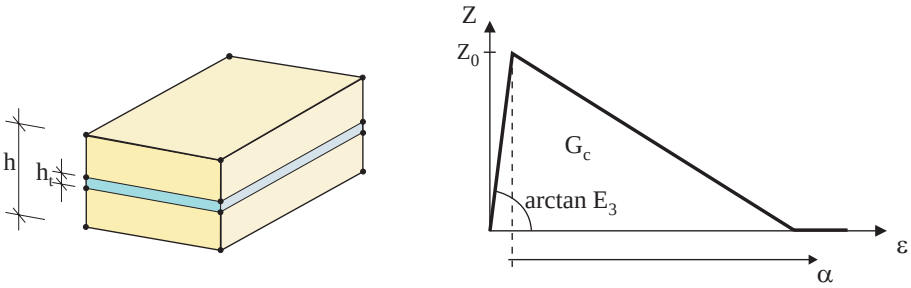

Figure 1. *Interface layer and softening function*

In order to predict the location where delamination occurs the delamination criterion of Hashin [HAS80] is introduced. The application is restricted to small deformations. Therefore the criterion can be formulated using the Second Piola–Kirchhoff stress tensor:

$$\frac{(S^{33})^2}{Z_0^2} + \frac{(S^{13})^2 + (S^{23})^2}{R_0^2} \leq 1\,. \qquad [1]$$

Here, the interlaminar normal stresses S^{33}, the shear stresses S^{13} and S^{23}, the tensile strength in thickness direction Z_0 and the shear strength of the laminate R_0 enter into

equation (1). The stresses are given with respect to a local orthonormal coordinate system.

Furthermore, we introduce linear softening behaviour

$$Z(\alpha) = Z_0\,(1 - \mu\alpha) \geq 0 \qquad \text{with } \mu > 0\,, \qquad [2]$$

where the internal variable α denotes the equivalent inelastic strain. The critical energy release G_c rate corresponds to the area under the softening curve multiplied with h_t

$$G_c = \frac{Z_0^2 h_t}{2}\,(\frac{1}{E_3} + \frac{1}{Z_0\mu})\,, \qquad [3]$$

where E_3 denotes the elastic modulus in thickness direction. In the present model the energy is dissipated within the interface layer of thickness h_t, see Fig. 1.

If the elastic deformations are negligible, which means that the first term in the sum cancels out, the softening parameter μ can easily be determined from (3) as

$$\mu \;=\; \frac{Z_0\; h_t}{2\; G_c}\,. \qquad [4]$$

Delamination is defined, when the absolute value of the interlaminar stress vector vanishes.

2.2. *The rate–independent model*

The fracture criterion (1) is reformulated and extended by the softening function (2) as follows

$$F(\mathbf{S}, \alpha) = g(\mathbf{S}) - Z(\alpha) \qquad [5]$$

with

$$g(\mathbf{S}) = \sqrt{\mathbf{S}^T \mathbf{A} \mathbf{S}}\,, \qquad \mathbf{A} = \text{Diag}\left[0,\; 0,\; 1,\; 0,\; \left(\frac{Z_0}{R_0}\right)^2,\; \left(\frac{Z_0}{R_0}\right)^2\right]\,. \qquad [6]$$

The components of $\mathbf{S} = [S_{11}, S_{22}, S_{33}, S_{12}, S_{13}, S_{23}]^T$ and $\mathbf{A}$ refer to a local Cartesian coordinate system. For $\alpha = 0$ eq. (5) is another representation of (1).

For small strains the Green–Lagrange strain tensor $\mathbf{E} = \mathbf{E}^{el} + \mathbf{E}^{in}$ is additively decomposed in an elastic and an inelastic part. The elastic part follows from the linear constitutive law $\mathbf{E}^{el} = \mathbf{C}^{-1}\,\mathbf{S}$, where the constitutive tensor $\mathbf{C}$ in terms of the elasticity constants E_i, G_{ij} and ν_{ij} is described in Sprenger, Gruttmann and Wagner[SPR00]. The inelastic strain rates and the evolution law for the equivalent plastic strains are given with the inelastic multiplier $\dot{\lambda}$, thus

$$\dot{\mathbf{E}}^{in} = \dot{\lambda}\,\mathbf{N}\,, \qquad \dot{\alpha} = \dot{\lambda}\,. \qquad [7]$$

The gradient of the yield function can be expressed as $\mathbf{N} = \mathbf{A}\,\mathbf{S}/g$. Finally the loading–unloading conditions must hold

$$\dot{\lambda} \geq 0\,, \quad F \leq 0\,, \quad \dot{\lambda} F = 0\ . \tag{8}$$

In case of loading with $\dot{\lambda} > 0$ the rate equations (7) are approximately integrated in time using a backward Euler integration algorithm. Within a time step $t_{n+1} = t_n + \Delta t$ one obtains, after some algebraic manipulations, the stress tensor and the parameter α

$$\mathbf{S}_{n+1} = \mathbf{P}\,\mathbf{E}^{tr}\,, \qquad\qquad \alpha_{n+1} = \alpha_n + \lambda\,, \tag{9}$$

with $\mathbf{P} = [\mathbf{C}^{-1} + \frac{\lambda}{Z}\,\mathbf{A}]^{-1}$ and $\mathbf{E}^{tr} = \mathbf{E}_{n+1} - \mathbf{E}_n^{pl}$. Here, the abbreviations $\lambda := \Delta t \dot{\lambda}_{n+1}$, $\mathbf{S}_{n+1} = \mathbf{S}(t_{n+1})$ and $\alpha_{n+1} = \alpha(t_{n+1})$ are introduced.

Linearization of the stress tensor yields the consistent tangent tensor

$$\bar{\mathbf{D}} = \mathbf{P} - \frac{\mathbf{P}\mathbf{N} \otimes \mathbf{P}\mathbf{N}}{\mathbf{N} \cdot \mathbf{P}\mathbf{N} + H} \qquad , \qquad H = \frac{Z'}{1 - \lambda \frac{Z'}{Z}}\,, \tag{10}$$

with $Z' := \mathrm{d}Z/\mathrm{d}\alpha$. If for $Z > 0$ the softening parameter μ increases certain values, negative diagonal terms in $\bar{\mathbf{D}}$ occur. In this case the global iteration process to solve the equilibrium equations becomes unstable. For $Z = 0$ the expressions for $\mathbf{P}$ and H are undefined. This can be avoided introducing a tolerance.

2.3. *Viscoplastic regularization*

To prevent the described numerical instabilities, we use a regularization technique. The viscoplastic strain rates are introduced according to the approach of Duvaut and Lions [DUV72]

$$\begin{aligned} \dot{\mathbf{E}}^{in} &= \dot{\mathbf{E}}^{vp} = \frac{1}{\eta}\mathbf{C}^{-1}\left(\mathbf{S} - \bar{\mathbf{S}}\right)\,, \\ \dot{\alpha} &= -\frac{1}{\eta}\left(\alpha - \bar{\alpha}\right)\,, \end{aligned} \tag{11}$$

where η denotes the viscosity parameter. Here, η is a numerical parameter which has the meaning of a relaxation time. The stresses $\bar{\mathbf{S}}$ and equivalent plastic strains $\bar{\alpha}$ denote the solutions of the rate–independent theory.

Substitution of eq. $(11)_1$ into the additive decomposition the strain rates yields with the elastic constitutive law

$$\begin{aligned} \dot{\mathbf{S}} + \frac{1}{\eta}\mathbf{S} &= \mathbf{C}\,\dot{\mathbf{E}} + \frac{1}{\eta}\bar{\mathbf{S}}\,, \\ \dot{\alpha} + \frac{1}{\eta}\alpha &= \frac{1}{\eta}\bar{\alpha}\,. \end{aligned} \tag{12}$$

The homogeneous differential equations can be solved in an exact way. Against it the inhomogeneous solution is obtained approximately using a backward Euler integration

procedure. Thus, introducing $\mathbf{S}_n = \mathbf{S}(t_n)$, $\delta = \Delta t/\eta$ and $\beta = \exp(-\delta)$ we end up with

$$\begin{aligned} \mathbf{S}_{n+1} &= \beta\,\mathbf{S}_n + (1-\beta)\,\bar{\mathbf{S}}_{n+1} + \frac{1-\beta}{\delta}\,\mathbf{C}\,\Delta\mathbf{E}\,, \\ \alpha_{n+1} &= \beta\,\alpha_n + (1-\beta)\,\bar{\alpha}_{n+1}\,. \end{aligned} \qquad [13]$$

The viscoplastic tangent matrix follows immediately with

$$\mathbf{D} = \frac{\mathrm{d}\mathbf{S}}{\mathrm{d}\mathbf{E}} = \frac{1-\beta}{\delta}\,\mathbf{C} + (1-\beta)\,\bar{\mathbf{D}}\,. \qquad [14]$$

The first term in (14) leads to positive diagonal entries in the viscoplastic tangent matrix, where the factor δ implies that with decreasing η the time increment Δt has to be reduced, to obtain the desired effect. The symmetric matrix $\mathbf{D}$ is necessary to setup the tangent stiffness matrix for the equilibrium iteration.

3. Examples

3.1. *Delamination of a sublayer in a plate strip*

The stability behaviour of a plate strip with an assumed fixed delamination zone has been investigated in Gruttmann and Wagner [GRU94] and Sprenger et al. [SPR00]. In this paper we consider the same example, however with a propagating delamination zone. The geometrical data and the material properties are shown in Fig. 2.

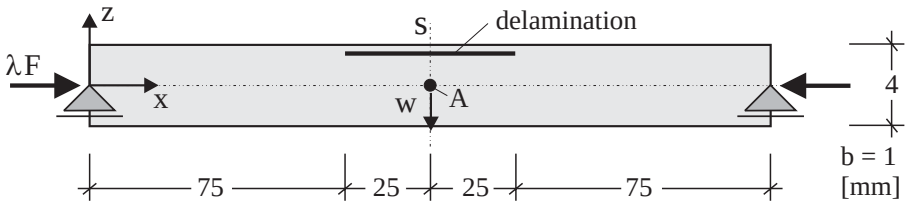

$$\begin{array}{rclrcl} E_1 &=& 137900\ N/mm^2 & G_{12} &=& 5860\ N/mm^2 \\ E_2 &=& 14480\ N/mm^2 & G_{23} &=& 5860\ N/mm^2 \\ \nu_{12} &=& 0.25 & F &=& 50\ N \end{array}$$

Figure 2. *Delaminated plate strip: geometry and material data*

The plate strip consists of 10 layers and the assumed delamination zone lies between layer 9 and 10 in the range $75 \le x \le 125$ mm, see Fig. 2. The fiber orientation is described within a symmetric stacking sequence $[0°/90°/0°/90°/0°]_s$, where $0°$ refers to the x-direction.

In Fig. 3 the finite element mesh is shown. Due to symmetry only half of the system is discretized. Different mesh densities are chosen. Here, we introduce with

n_1, n_2, n_3 the number of elements in length direction in the depicted ranges. The interface layer with thickness h_t is arranged between layer 9 and 10 in the interval of L_2. In the range of L_3 delamination is not possible. The discretization in y–direction and z–direction is performed with one and four elements, respectively. The external load is applied via rigid elements. A finite element mesh with $n_1 = 12$, $n_2 = 24$ and

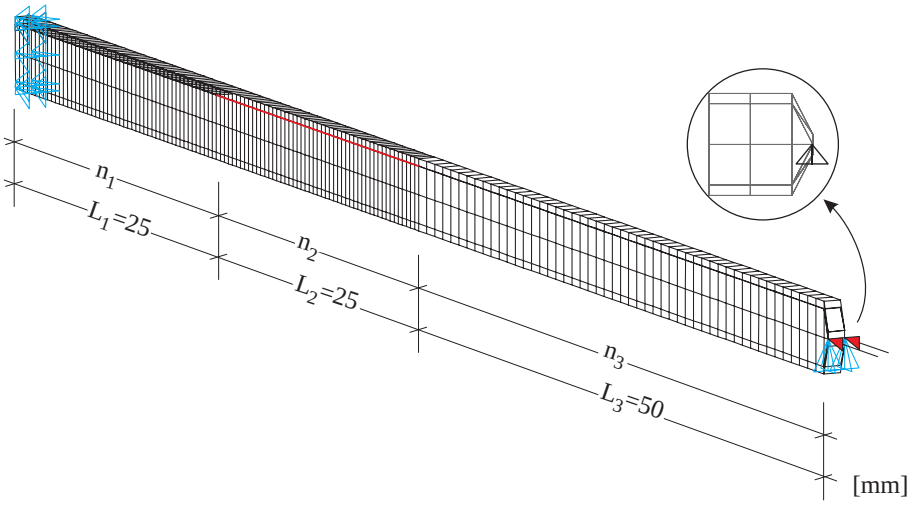

Figure 3. *Delaminated plate strip: finite element mesh*

$n_3 = 24$ is chosen for the numerical calculations. Two deformed configurations with buckled sublaminates are plotted in Fig. 4. The length of the delamination zone L_{del} remains constant and is given in the first case with $L_{del} = L_1 = 25\,mm$ and in the second case with $L_{del} = L_1 + L_2 = 50\,mm$ for half the system, respectively. Thus, the associated computed load deflection curves represent lower and upper bounds for the subsequent delamination analysis, see Figs. 5 - 6. The external load is increased until the delaminated layer buckles. An imperfection is imposed automatically on the system due to the non-uniform discretization in z–direction. Thus, with increasing load the plate switches into the secondary solution path without further perturbation. The structure with the short delamination zone $L_{del} = 25\,mm$ yields the higher carrying load. All calculations are done controlling the axial displacement at the support. In the following we discuss a variation of the parameters μ and h_t. Here, we choose $n_1 = n_2 = n_3 = 50$ and numerical strength parameters $Z_0 = 0.42\,N/mm^2$, $R_0 = 6.0\,N/mm^2$. In Fig. 5 the load factor λ versus the transverse displacement w of point A is depicted. The curves for the propagating delaminations using four different softening parameters are enveloped by the solutions with fixed delamination lengths, as mentioned before. The softening parameter μ is inversely proportional to the critical energy release rate G_c. Thus with increasing μ the delamination zone propagates faster. Using a parameter $\mu \geq 0.75$, the delamination develops all over the total range L_2 and the load displacement curve approaches the lower limit curve. The influence of h_t on the global deformation behaviour is for this example practically negligible,

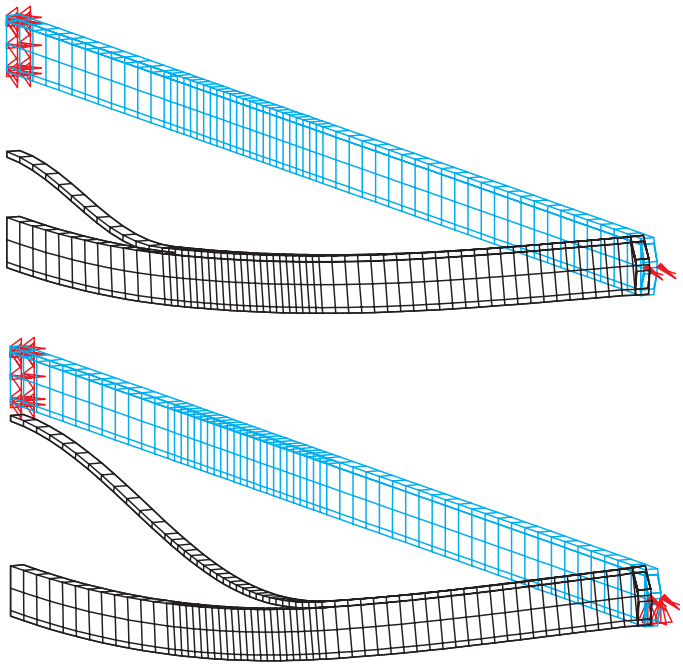

Figure 4. *Delaminated plate strip: deformed meshes with short and long delamination zone*

as can be seen in Fig. 6. Furthermore, it has been shown that a numerical integration of the residual vectors and stiffness matrices using four integration points is sufficient for the relative thin interface layers.

Deformed meshes at different load levels are plotted in Fig. 7. Finally, we define the following parameter

$$D = 100\frac{Z_0 - Z(\alpha)}{Z_0} \qquad [15]$$

to illustrate the delamination progress. Here, $D = 100\,\%$ describes a total delamination which means that the absolute value of the interlaminar stress vector is reduced to zero. The plots show that the newly opened surfaces are completely free of stresses.

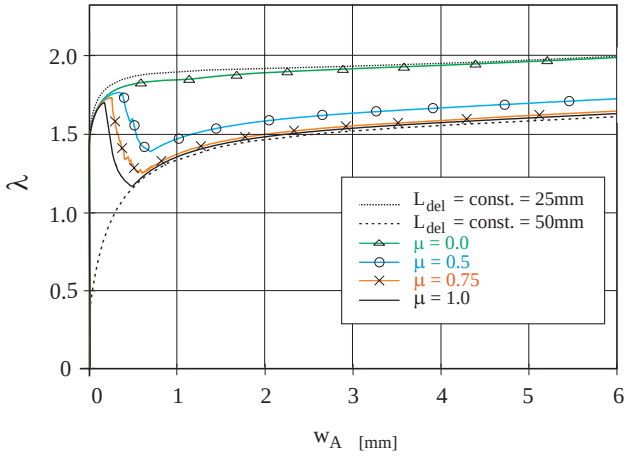

Figure 5. *Delaminated plate strip: variation of the softening parameter μ at constant thickness $h_t = 0.02\,mm$*

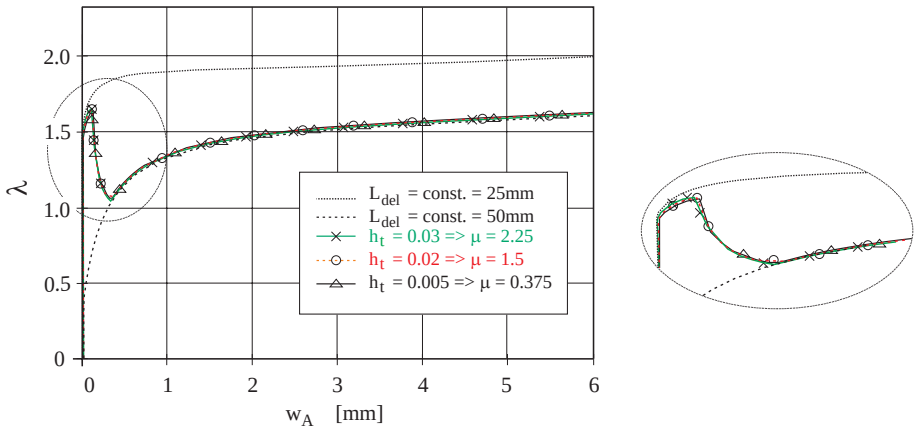

Figure 6. *Delaminated plate strip: variation of the thickness h_t at constant energy release rate G_c*

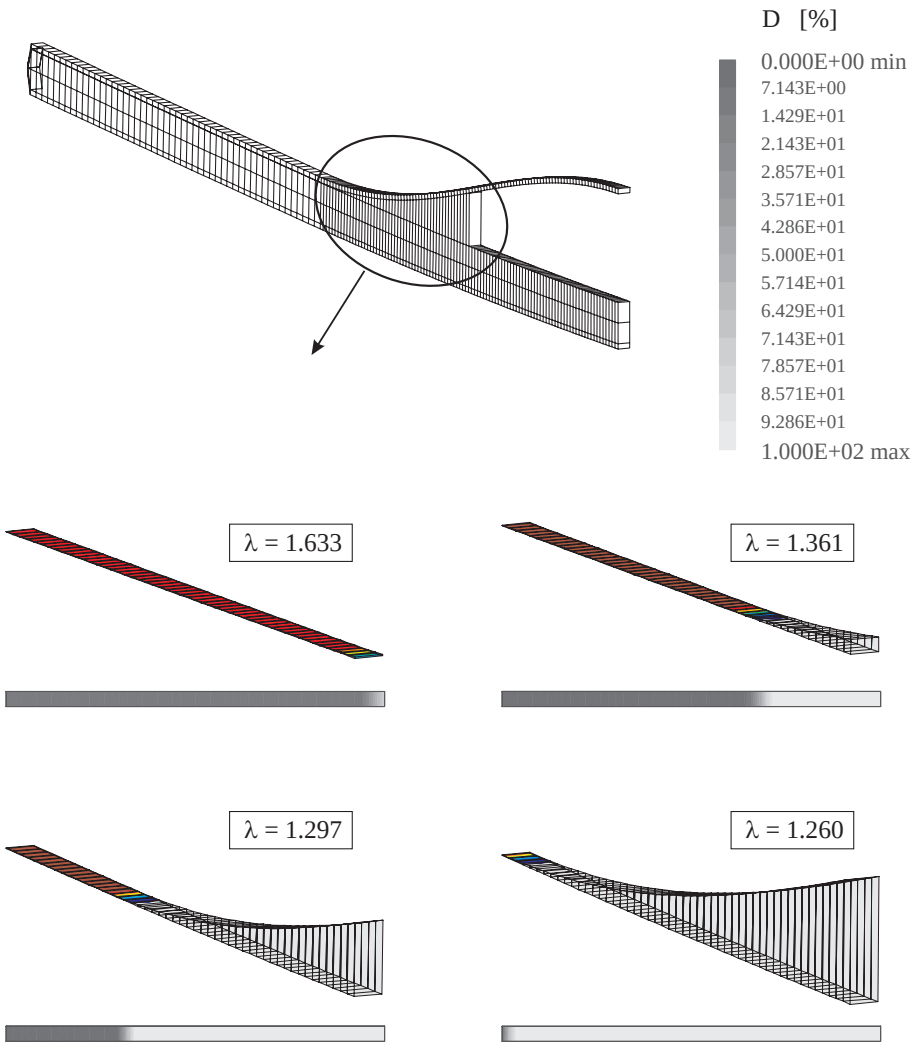

Figure 7. *Delaminated plate strip: delamination growth for different load factors* λ *and constant* $\mu = 1.5$

3.2. *Initial circular delamination in a plate*

In the next example we discuss the nonlinear behaviour of a plate under axial loads. The plate consists of 16 layers with a layer thickness $h_L = 0.12\,mm$ and stacking sequence $[0°/0°/+45°/0°/0°/-45°/0°/90°]_S$. Again an unsymmetric delamination is introduced. Here, we choose a circular delamination between layer 14 and 15, see Fig. 8. The plate is simply supported along the edges. The geometrical data and the material data for an AS/3501 graphite epoxy composite are given as follows:

$$\begin{array}{rclrrclr} E_1 & = & 135000 & N/mm^2 & G_{12} & = & 5150 & N/mm^2 \\ E_2 & = & 8500 & N/mm^2 & G_{23} & = & 5150 & N/mm^2 \\ \nu_{12} & = & 0.317 & & & & & \\ Z_0 & = & 51.7 & N/mm^2 & R_0 & = & 91.0 & N/mm^2 \\ h_t & = & 0.005 & mm & F & = & 30 & N/mm \end{array} \qquad [16]$$

The $\pm 45°$ layers lead to a non-symmetric behaviour of the structure. Thus symmetry with respect to the x-axis and y–axis is not given. Nevertheless this fact is ignored in the present analysis to reduce the computational effort.

The stability behaviour of this structure has been investigated by Cochelin et.al. [COC94] for the case of nongrowing delaminations. In the present paper we study the influence of propagating delaminations. Thus, we introduce interface elements between layers 14 and 15 in the fine discretized annular space. In thickness direction several physical layers are summarized within one element layer. This has to be considered when performing the numerical integration in thickness direction[KLI99]. The load parameter λ is used to control the nonlinear calculations. For comparisons, we analyze a "perfect" plate without delamination and the same plate with an artificial non–growing delamination zone. In the first case only in-plane loading occur due to the symmetric layup. With increasing axial deformation a bifurcation point is found at a load factor $\lambda = 50.3$. Based on a classical perturbation with the first eigenvector a switch to the secondary solution path is possible, see Fig. 10. Due to the eccentric position of the delamination zone an imperfect system is computed in the second case. One obtains a non-linear load displacement curve which approaches for large displacements the secondary solution path of the perfect plate. In the following, we discuss the effects of a propagating delamination zone. Here we investigate the influence of the softening parameter μ and the size of the time step Δt. The load deflection curves in Fig. 9 show the variation of the softening parameter μ, and thus the influence of G_c for propagating delaminations. A parameter $\mu = 0.58$ corresponds to an energy release rate $G_c = 0.222 N/mm$, see eq. (4), which is a realistic value. The largest value of $\mu = 0.88$ corresponds to $G_c = 0.147 N/mm$. Noticeable differences occur in the range of moderate displacements. This is due to the fact that for finite deformations global buckling dominates the behaviour. The influence of two different time steps Δt is depicted in Fig. 10. Only minor differences can be seen.

Delamination starts at the coordinates $(x = 0\,mm, y = 5\,mm)$ and propagates along the inner circle. With increasing load a second point with coordinates $(x =$

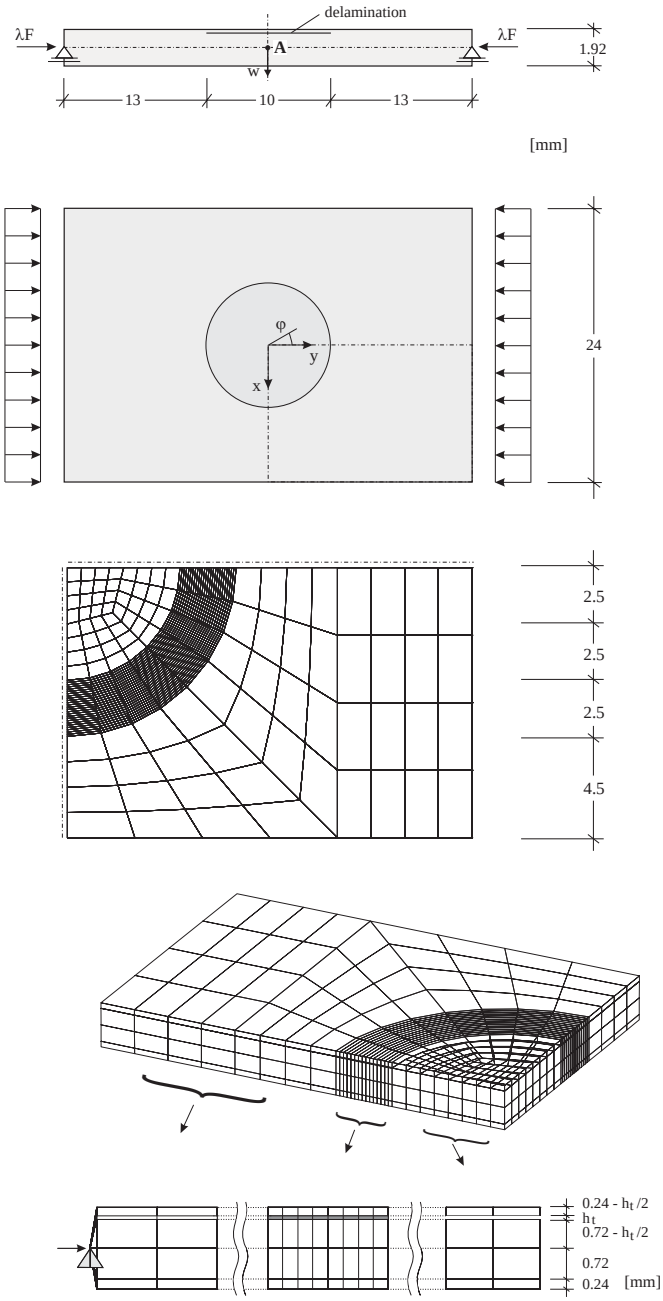

Figure 8. *Plate with circular delamination: geometry and finite element mesh*

$5\,mm, y = 0\,mm)$ becomes critical. Hence, both delamination ranges fuse. The whole process is depicted in Fig. 11.

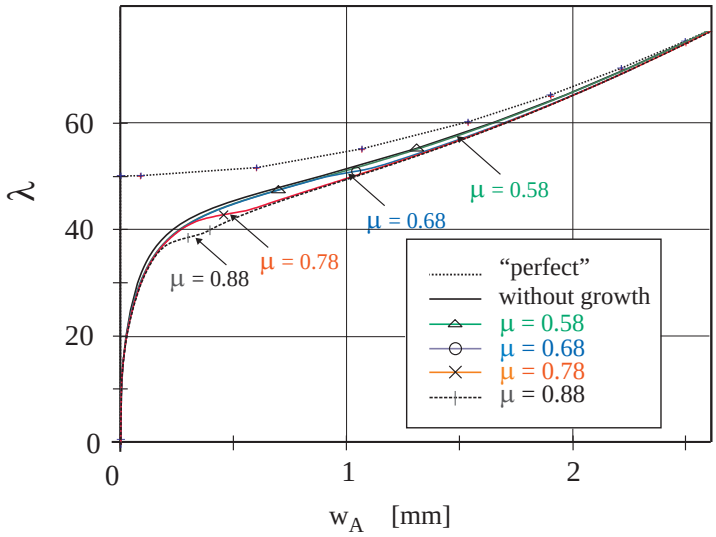

Figure 9. *Variation of the softening parameter μ with constant $\Delta t = 0.1$*

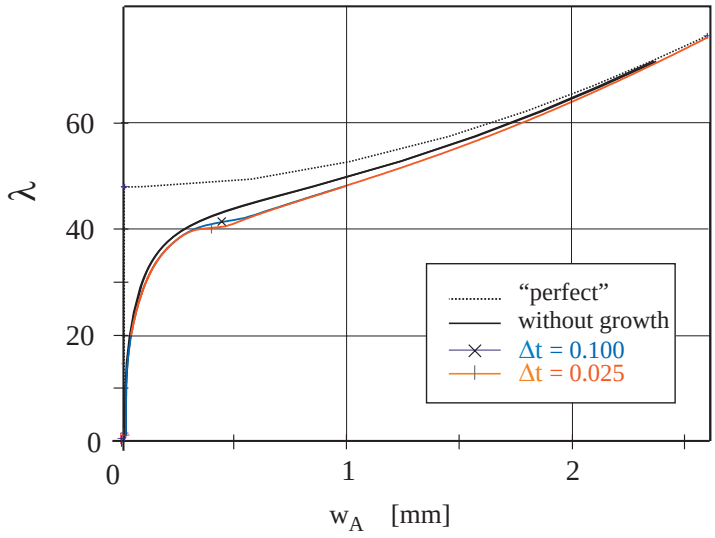

Figure 10. *Variation of the time step Δt with constant $\mu = 0.78$*

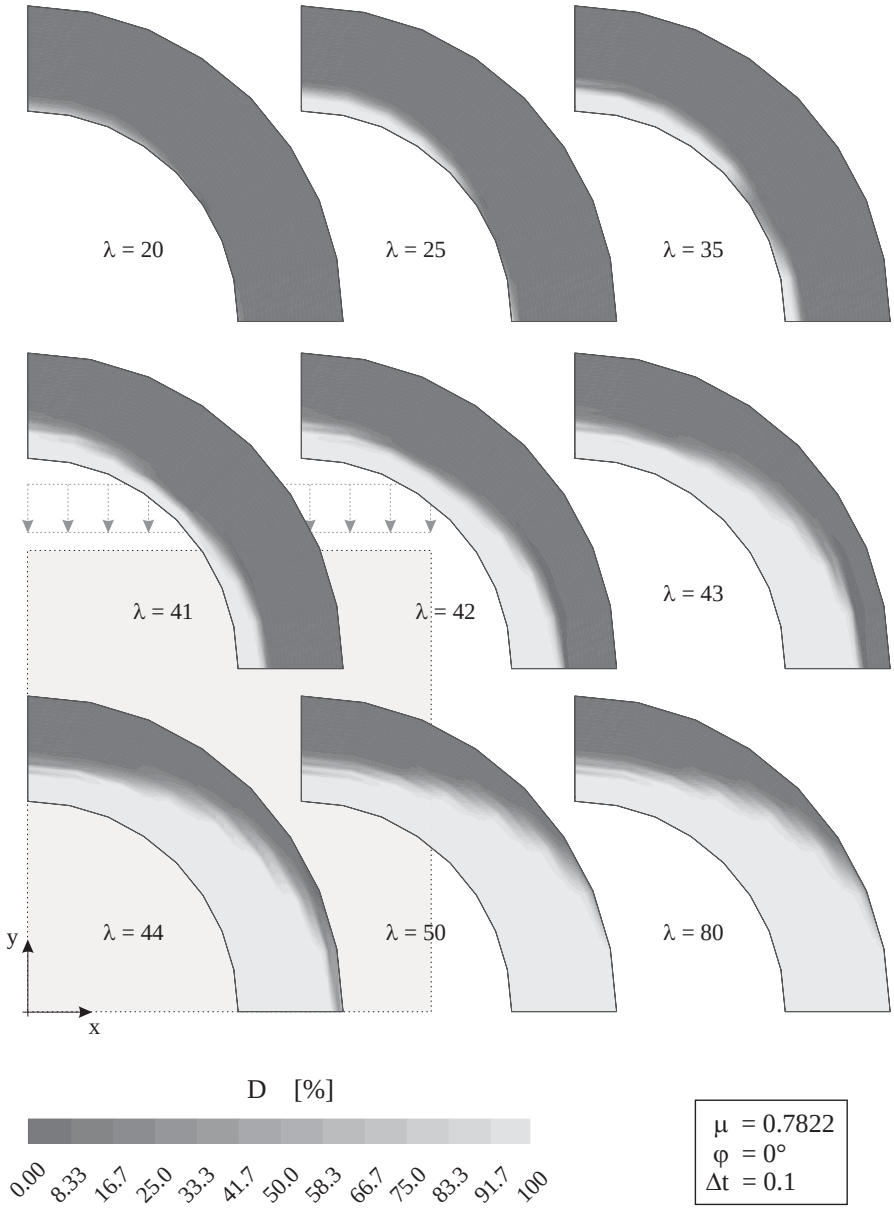

Figure 11. *Growing delamination zone*

4. Conclusions

In this paper a model to simulate increasing delaminations in composite structures within a finite element approach is presented. Interface elements with small but non–vanishing thickness are developed using refined hexahedral elements. These elements are located in regions where delaminations are expected. Within an inelastic model, the delamination criterion of Hashin is extended to a yield criterion with softening. A viscoplastic regularization procedure is introduced to avoid numerical instabilities. The viscosity parameter is determined such that the critical energy release rate is the essential material parameter. Detailed numerical calculations show the robustness and reliability of the developed delamination model within a stability analysis.

5. References

[BET95] BETSCH P., STEIN E., *An Assumed Strain Approach Avoiding Artificial Thickness Straining for a Nonlinear 4-Node Shell Element*, Communications in Numerical Methods in Engineering. vol. 11, num. 1995, p. 899-910.

[COC94] COCHELIN B., DAMIL N., POTIER-FERRY M., *Asymptotic-Numerical Methods and Padé Approximants for Nonlinear-Elastic Structures*, International Journal for Numerical Methods in Engineering. vol. 37, num. 1994, p. 1137-1213.

[CRIS97] CRISFIELD M.A., JELENIC G., MI Y., ZHONG H.G., FAN Z., *Some Aspects of the Non-linear Finite Element Method*, Finite Elements in Analysis and Design. vol. 27, num. 1997, p. 19-40.

[DUV72] DUVAUT G., LIONS J.L., *Les Inequations en Mechanique et en Physique*, Dunod, Paris, 1972.

[BAT84] DVORKIN E., BATHE K.J., *A Continuum Mechanics Based Four Node Shell Element for General Nonlinear Analysis*, Engineering Computations. vol. 1, num. 1984, p. 77-88.

[GRU94] GRUTTMANN F., WAGNER W., *On the Numerical Analysis of Local Effects in Composite Structures*, Composite Structures vol. 29, num. 1994, p. 1-12.

[HAS80] HASHIN Z., *Failure Criteria for Unidirectional Composites*, Journal of Applied Mechanics. vol. 47, num. 1980, p. 329-334.

[KLI99] KLINKEL S., GRUTTMANN F., WAGNER W., *A Continuum Based Three-Dimensional Shell Element for Laminated Structures*, Computers & Structures. vol. 71, num. 1999, p. 43-62.

[SCH94] SCHELLEKENS J.C., DE BORST R., *Free Edge Delamination in Carbon-Epoxy Laminates: A Novel Numerical/Experimental Approach*, Composite Structures. vol. 28, num. 1994, p. 357-373.

[SPR00] SPRENGER W., GRUTTMANN F., WAGNER W., *Delamination growth analysis in laminated structures with continuum based 3D-shell elements and a viscoplastic softening model*, Computer Methods in Applied Mechanics and Engineering. vol. 185, num. 2000, p. 123-139.

[WAN85] WANG A.S.D., SLOMIANA M., BUCINELL R.B., "Delamination Crack Growth in Composite Laminates", *Delamination and Debonding of Materials*, Philadelphia, 1995, ASTM, p. 135-167.